



the society for solid-state
and electrochemical
science and technology

ECS Solid State Letters

Ballistic Electron Emission Microscopy Study of Charge Transport Across an Au/Graphene-Oxide/Modified-Si Stack

R. S. Kajen, N. Chandrasekhar, Ming Hua Ng, Seok Hong Goh, Kin Leong Pey and C. Vijila

ECS Solid State Lett. 2012, Volume 1, Issue 2, Pages M13-M15.
doi: 10.1149/2.013202ssl

Email alerting service

Receive free email alerts when new articles cite this article - sign up in the box at the top right corner of the article or [click here](#)

To subscribe to *ECS Solid State Letters* go to:
<http://ssl.ecsdl.org/subscriptions>

© 2012 The Electrochemical Society



Ballistic Electron Emission Microscopy Study of Charge Transport Across an Au/Graphene-Oxide/Modified-Si Stack

R. S. Kajen,^{a,b} N. Chandrasekhar,^c Ming Hua Ng,^a Seok Hong Goh,^a Kin Leong Pey,^{b,*} and C. Vijila^{a,z}

^aInstitute of Material Science and Engineering, Singapore 117602

^bDivision of Microelectronics, School of Electrical and Electronic Engineering, Nanyang Technological University, Singapore 639798

^c19th Cross, Malleswaram, Bangalore 560 055, India

Ballistic electron emission microscopy/spectroscopy (BEEM/S), a three-terminal scanning tunneling microscopy (STM) technique is used to study charge transport across an Au/graphene-oxide/modified-silicon (Au/GO/m-Si) stack with nanoscale resolution. The Au/GO interface is found to be non-homogeneous with an average injection barrier of 1.0 eV for electrons and 0.5 eV for holes. These measurements will be useful for device design in the area of graphene-related electronics.
 © 2012 The Electrochemical Society. [DOI: 10.1149/2.013202ssl] All rights reserved.

Manuscript submitted April 11, 2012; revised manuscript received May 22, 2012. Published July 20, 2012.

The absence of a finite bandgap¹ in graphene has led to the emergence of a whole array of functionalized graphene materials. Amongst these functionalized graphene materials, graphene-oxide² with a tunable bandgap, is seen as a promising route toward solution processable³ large-scale graphene electronics. However, GO itself has been labeled as an insulator⁴ and almost never used directly in an electronic device without prior chemical reduction. Studies involving GO or reduced-GO (r-GO) have been largely concerned with charge transport along the GO (parallel to the graphene basal plane).⁵ Literature discussing transport in the vertical direction through GO⁶ is scarce. In this work, we employ ballistic electron emission microscopy (BEEM),⁷ a three-terminal scanning tunneling microscopy (STM) technique to investigate the vertical transport across a metal/graphene-oxide/modified-Si (Au/GO/m-Si) stack structure. Being an STM-based technique the method is capable of measuring electron/hole injection barrier heights with nanoscale spatial resolution and 6 meV energy resolution at liquid nitrogen temperature (77 K).⁸ In addition, as there is no bias across the device, it rules out the possibility of a large electric field build up across the BEEM device, thereby enabling measurements with low perturbation to the system.

Experimental

The graphene-oxide (GO) solution used in this work was prepared by a modified-Hummers method.⁹ Atomic force microscopy (AFM) measurements were carried using multimode Digital Instruments system in the tapping mode to characterize the GO layers obtained from the solution. The GO solution was drop-casted on a Si sample with a layer of 300 nm thick SiO₂ pre-treated with amino-propyl-triethoxysilane (APTES) to promote adhesion of the GO-flakes. Coarse inspection of the presence of GO flakes was carried out via an optical microscope. Thereafter, the sample was analyzed by AFM. Fig. 1a shows information on the position of GO flakes in a 10 μm by 10 μm area. To verify the existence of single/double layer GO flakes, a line profile (see vertical dashed line) over a potential region (circled in red) was taken, as depicted in the inset of Fig. 1a. The height of the single and double flake was measured to be 0.8 and 1.7 nm, respectively. The measured heights are in good agreement with reported results found in the literature.¹⁰ Raman spectroscopy (WITec CRM200 system with wavelength 488 nm and spot size ~0.5 μm) was used to verify the presence of graphene oxide. Fig. 1b is the Raman spectrum obtained from a GO coating patterned onto a 2 μm grating. Three peaks were observed at 1354 cm⁻¹, 1595 cm⁻¹ and 2700 cm⁻¹ from the spectra (see inset for zoomed-in view). These peaks represent the D, G and 2D peaks respectively, validating the presence of GO¹¹ in the solution used for coating.

In a typical BEEM experiment, represented by Fig. 2a, the semiconducting layer (GO) is deposited on the collector (n-type ion implanted silicon), and overlaid with a metallic layer as a top electrode (base). By controlling the STM tip above the top electrode, spectroscopic measurements of injection barriers between the top metal and the semiconducting layer are possible, as well as imaging of charge transport through the semiconductor material. The tips used were Pt-Ir, which were manually snapped off from Pt-Ir wire. They were chemically cleaned with standard solvents prior to use. Such tips are relatively inert to oxidation (when compared to W tips), and are therefore preferred for spectroscopic studies.

An n-type Si (111) wafer doped with phosphorous at 10¹⁵ cm⁻³ was ion-implanted with arsenic at the back of the wafer. The wafer was then subjected to a rapid thermal annealing (RTA) process at 1000°C for 3 s to activate the implanted ions. The wafer was then diced into 6 × 6 mm² square samples and cleaned by acetone for 10 minutes followed by an IPA (iso-propyl alcohol) clean for 10 minutes. Thereafter the samples were subjected to a 20 second dip in 7% buffered Hydro-Fluoric acid (HF), followed by a dip into deionized (DI) water to check for hydrophobicity. The cleaned sample was then dipped in a 2% aqueous APTES solution for 2 minutes, rinsed in DI water and blown dry with N₂. The GO solution was then dropped casted onto the APTES treated Si surface (m-Si). After 1 min, the samples were then quickly rinsed in DI water, blown-dry with nitrogen gas, immediately transferred into a thermal evaporator and placed under vacuum conditions. The APTES layer is estimated to be 1 monolayer in thickness.¹² A 10 nm thick layer of gold (99.9% purity) was thermally evaporated at 10⁻⁵ Pa at a deposition rate of 0.1 Å/s through a shadow mask (5×5 array of disks with diameter of 0.5 mm) to form the BEEM device shown in Fig. 2a. The sample temperature was monitored with a thermocouple mounted on the sample holder. The temperature of this stayed below 50°C, thereby precluding the possibility of GO reduction, which is known to occur above 100°C.¹³

The sample was then probed at various locations by BEEM spectroscopy to find a suitable location and bias for imaging. Fig. 2b is the STM image obtained by scanning the tip at a constant voltage bias of -1.2 V. Fig. 2c maps the BEEM current through the sample at -1.2 V. The BEEM image reveals that the GO/Au barrier is non-homogeneous, and can be separated into 3 distinct regions labeled 1-3. To further probe the barrier heights in the 3 regions, BEES spectra at a constant tunneling current of 1 nA was obtained from the 3 regions as shown in Fig. 2d.

Discussion

The barrier heights extracted using the Bell-Kaiser (B-K) model¹⁴ were found to be 0.8, 0.9 and 1.0 eV for regions 1, 2 and 3, respectively. We infer that the 3 regions that we see are attributable to multi-layer GO, double-layer GO and single layer GO respectively. This correlates

*Electrochemical Society Active Member.

^zE-mail: eklpey@ntu.edu.sg; c-vijila@imre.a-star.edu.sg

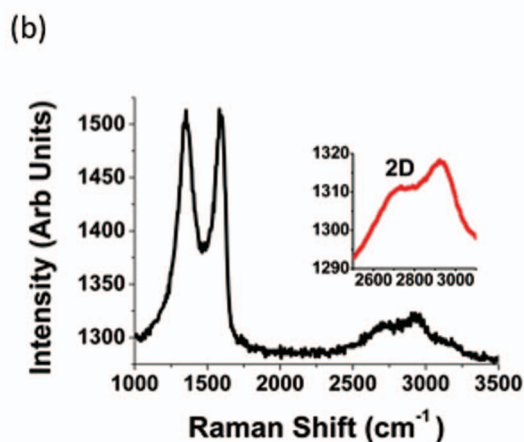
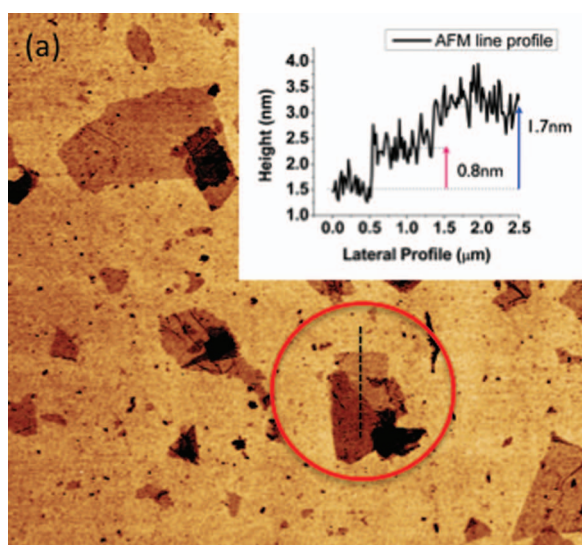


Figure 1. (a) Atomic force microscopy image of GO on 300 nm SiO₂/Si. The presence of single/double layer GO was confirmed via the height profile (see inset) along the dashed line within the circled GO region. (b) Raman spectroscopy analysis on a GO coating detects the D, G and 2D peaks. A zoomed-in view of the 2D peak is shown in the inset for clarity.

quite well with the AFM results presented in Fig. 1a. Such an inference is justifiable, since it is an elementary result of tight binding that the bandgap reduces as the number of atoms/layers increases. However, we do acknowledge the possibility of region 1 being a GO-deficient area, leading to an Au/Si barrier of 0.8 eV. The presence of three such distinct regions (single layer GO, double layer GO and multi-layer or no GO), gives a distribution of barrier heights. It is also possible that the barrier height fluctuations are due to changes in the density of states of graphene oxide caused by the presence of various functional groups (defects) on the graphene basal plane. To obtain the statistical distribution of the barrier height, the BEEM spectra were taken over several locations at a constant tunneling current of 0.5 nA. Fig. 3a shows BEES/BHES B-K fits to an average of over 10 spectra. From the fitting, an electron/hole barrier height of 1.0/0.5 eV is obtained. The distribution of the barrier height extracted using the B-K model for electron injection and hole injection are represented in Figs. 3b and 3c respectively. The histograms support the findings obtained from the Fig. 3a.

However, in the strictest sense, neither the Bell-Kaiser, nor wavevector-dependent (*k*-dependent) BEEM theories can be directly applied for a disordered organic material (GO), where *k* is not a good quantum number. In the absence of a BEEM theory for such materials, the next best option is to read off the threshold from the point where the BEEM current deviates from zero,¹⁵ addressed henceforth as the “inspection method”. We find that in our work, the inspection method gives similar injection barriers as those extracted using the B-K model.

BEEM experiments (not shown here) on Au/APTES/Si structures have confirmed that the APTES layer has a negligible effect in modifying the Au/Si Barrier height (0.8/0.3 eV for electron/holes respectively). Therefore we conclude that the APTES layer acts mainly as an adhesion promoter and does not lead to an additional transport barrier. Hence, carriers are injected ballistically only into the Au. They traverse the Au, and enter the GO by crossing the Au-GO barrier. Only electrons/holes that cross the Au/GO barrier, and overcome the Si conduction/valence bands respectively will be collected as BEEM current. Hence, the silicon collector sets up a lower limit of the measured barriers as it will block carriers, which have lower injection barriers than the Au/Si electron/hole injection barrier heights of 0.8/0.3 eV respectively. Recent photo capacitance measurements by Bansal et al. support the existence of the 1.0 eV and -0.5 eV state with reference to the Fermi level of GO.¹⁶

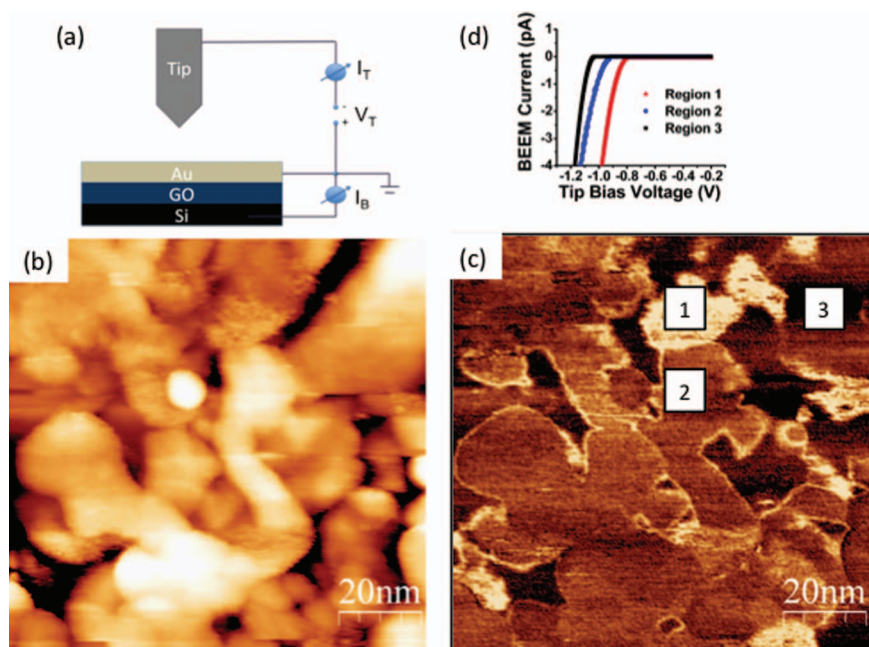


Figure 2. (a) Schematic of the ballistic electron emission microscopy (BEEM) experimental setup. (b) Scanning tunneling microscopy image of the top gold surface under a tip bias of -1.2 V and 1 nA tunneling current. (c) BEEM image of the Au/GO interface on a 100×100 nm² area scanned at a constant tip bias of -1.2 V. A current range of 12 pA has been used to enhance the contrast. The darker areas correspond to lower BEEM current and lighter areas to higher BEEM current. Three distinct regions labeled 1–3 have been found. (d) Ballistic Electron Emission Spectroscopy (BEES) at the 3 regions shown in (c) at a constant tunneling current of 1 nA confirms the presence of 3 different barrier heights at the interface. The spectroscopy is in agreement with the barrier height trend observed from imaging.

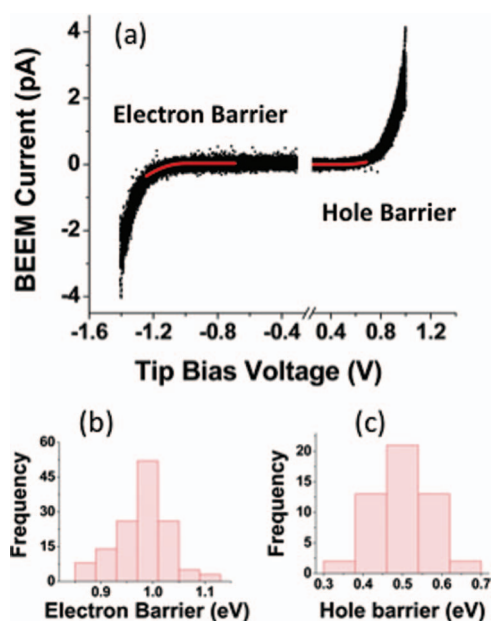


Figure 3. (a) The BEES (left) and BHES (right) spectra at a constant tunneling current of 0.5 nA. Both curves are obtained from an average of 9 or more spectra. Electron/hole barrier heights of 1.0 eV/0.5 eV were extracted by fitting the curves to the Bell-Kaiser model as shown in red. (b) and (c) Distribution of the electron and hole barrier heights, respectively, obtained via BEES/BHES at various locations.

First measurements on the Au/GO injection barrier were done by Wu et al.¹⁷ There are two key differences between our experiment (BEEM) and this work (*I-V* measurement). *I-V* is known to measure the minimum injection barrier, yielding the smaller of either the electron or hole barrier. BEEM measures the electron and the hole barriers independently. In addition, the nanoscale inhomogeneity could be mapped. Secondly in the (*I-V*) experiment, bottom contacts (Au) are used whereas in our case we had used top contacts. The bottom contact configuration is expected to cause significant bending of the GO sheets at the electrode edges, which is likely to introduce a local potential barrier.¹⁸ These significant differences preclude a direct comparison of our results with those of Wu et al. We have done similar *I-V* measurements and we have observed some features which

are similar and some which are different from those observed by Wu et al., which will be typically discussed in a separate paper since it is beyond the scope of the present work.

In conclusion, we report nanoscale inhomogeneities of the injection barrier at the Au/GO interface in an Au/GO/modified-Si stack using ballistic electron emission microscopy/spectroscopy. A distribution of injection barriers were found with an average electron/hole injection barrier of 1.0 eV and 0.5 eV respectively. The barrier height spread is likely to be due to different functional groups/defects on the graphene plane and GO thickness variations (single/double/multi layer GO), which cause local variations in the GO density of states/bandgap. Our measurements correlate well with the GO density of states reported by Bansal et al.¹⁶

This work is supported by SSDA (A-STAR). The authors would like to thank Johnson Goh, Cedric Troadec and Qin Hailang for technical discussions on BEEM.

References

1. G. Eda, G. Fanchini, and M. Chhowalla, *Nature Nanotechnology*, **3**, 270 (2008).
2. A. K. Geim, *Science*, **324**, 1530 (2009).
3. V. C. Tung, M. J. Allen, Y. Yang, and R. B. Kaner, *Nature Nanotechnology*, **4**, 25 (2009).
4. K. A. Mkhoyan, A. W. Contryman, J. Silcox, D. A. Stewart, G. Eda, C. Mattevi, S. Miller, and M. Chhowalla, *Nano Letters*, **9**(3), 1058 (2009).
5. C. G. Navarro, R. T. Weitz, A. M. Bittner, M. Scolari, A. Mews, M. Burghard, and K. Kern, *Nano Letters*, **7**(11), 3499 (2007).
6. Y. Kanamori, S. Obata, and K. Saiki, *Chemistry Letters*, **40**, 255 (2011).
7. W. J. Kaiser and L. D. Bell, *Physical Review Letters*, **60**, 1406 (1988).
8. V. Narayanamurti and M. Kozhevnikov, *Physics Reports*, **349**, 447 (2001).
9. Y. Y. Lee, S. L. Chong, S. H. Goh, M. H. Ng, M. V. Kunnavaakkam, C. L. Hee, Y. Xu, H. Tintang, C. Y. Su, and L. J. Li, *Journal of Vacuum Science and Technology B*, **29**, 011023 (2011).
10. S. Gilje, S. Han, M. Wang, K. L. Wang, and R. B. Kaner, *Nano Letters*, **7**(11), 3394 (2007).
11. K. N. Kudin, B. Ozbas, H. C. Schniepp, R. K. Prud'homme, I. A. Aksay, and R. Car, *Nano Letters*, **8**(1), 36 (2008).
12. J. Kim, P. Seidler, L. S. Wan, and C. Fill, *Journal of Colloid and Interface Science*, **329**(1), 114 (2009).
13. S. Stankovich, D. A. Dikin, R. D. Piner, K. A. Kohihaas, A. Kleinhammes, Y. Jia, Y. Wu, S. T. Nguyen, and R. S. Ruoff, *Carbon*, **45**, 1558 (2007).
14. M. Prietsch, *Physics Reports*, **253**, 163 (1995).
15. X. Feng, N. Chandrasekhar, H. Su, and K. Mullen, *Nano Letters*, **8**, 4259 (2008).
16. T. Bansal, A. D. Mohite, H. M. Shah, C. Galande, A. Srivastava, J. B. Jasinski, P. M. Ajayan, and B. W. Alphenaar, *Carbon*, **50**(3), 808 (2012).
17. X. Wu, M. Sprinkle, X. Li, F. Ming, C. Berger, and W. A. de Heer, *Physical Review Letters*, **101**, 026801 (2008).
18. A. B. Kaiser, C. Gomez-Navarro, R. S. Sundaram, M. Burghard, and K. Kern, *Nano Letters*, **9**(5), 1787 (2009).